RSC Advances

PAPER

View Article Online
View Journal | View Issue

Cite this: *RSC Adv.*, 2021, **11**, 7653

One-step sustainable synthesis of cationic high-swelling polymers obtained from starch-derived maltodextrins

Claudio Cecone, * Giulia Costamagna, Marco Ginepro and Francesco Trotta

Received 21st December 2020
Accepted 6th February 2021

DOI: 10.1039/d0ra10715h

rsc.li/rsc-advances

The good water solubility displayed by most starch-derived maltodextrins has limited their use when specific mechanical properties are required, particularly when working in aqueous media. As a result, numerous attempts to cross-link such polysaccharides to obtain cross-linked polymers have been reported; in this context, non-toxic and biocompatible water-soluble diglycidyl ethers have performed well. Besides, amines are commonly used as curing agents in combination with diglycidyl ethers for the production of epoxy resins. For this reason, amine-mediated epoxy ring-opening reactions of 1,4-butanediol diglycidyl ether have been studied as approaches to obtain sustainable cross-linked polymers suitable for eco-friendly scaling-up, based upon commercial starch-derived maltodextrins, using water as a unique solvent.

Introduction

Thermosets are plastics obtained from liquid monomers that irreversibly turn into solid products through polymerisation reactions. Thermosetting polymers make up less than 20% of global plastic production, whereas epoxy resins represent approximately 70% of the thermosets market.[1] Thanks to their good mechanical properties, chemical resistance and excellent adhesion characteristics even at high temperatures, epoxy resins have been used as coatings, laminates, adhesives, and in high performance composite production.[1,2] In this regard, diglycidyl ether bisphenol A (DGEBA) is used in approx. 90% of worldwide epoxy resin production. Despite the superior properties of DGEBA, the use of this epoxy monomer entails severe concerns related to its toxicity and petroleum-based nature.[3,4] For this reason, the development of bio-based epoxy resins obtained from renewable sources has attracted scientific and industrial attention, being compliant with the main aims of Green Chemistry.[5–9] In the production of epoxy resins, a key role is played by so-called curing agents, molecules whose task is to promote the cross-linking or curing of the polymer. For this reason, primary and secondary amines are commonly added to enhance the features of the final product.[10–12] Furthermore, tertiary amines and imidazoles have also been reported to act as curing agents, by initiating homo-polymerisation reactions.[13,14] As they are good nucleophiles, amines are known to react in a simple, effective, and environmentally friendly way with epoxides, giving β-hydroxyl amines as reaction products.[15] The amine–epoxide reaction is considered to be an example of "click" chemistry and, in the case of diglycidyl ether, it can lead to the generation of polymer structures, known as poly(β-hydroxyl amine)s.[16–19] The ring opening reaction is reported to occur either in organic solvent and water, characterised by the formation of zwitterion species in its first step;[20,21] by employing tertiary amines, positive charged quaternary ammonium functions were observed as a result.[22,23] Polysaccharides, owing to their biodegradability, biocompatibility and non-toxicity, have attracted increasing scientific and industrial interest over the past decade.[24,25] In this context, specific processes have allowed their structure to be functionalised with positive charges, obtaining cationic polymers.[26] These materials have been applied in industrial processes, *e.g.* as additives in the food and paper industries[25–27] and as green adsorbents and biocompatible superabsorbents for the treatment of waste waters in environmental applications.[28–30] Furthermore, they have been successfully applied in pharmaceutical and medical application, as drug delivery and gene delivery systems.[31–34] They have also been studied as scaffolds for tissue engineering applications.[33] Except for chitosan,[35] the main strategy reported for introducing positive charges involves the functionalisation of the polysaccharide backbone with specific molecules carrying quaternary ammonium groups. In this context, etherification with 2,3-epoxypropyltrimethylammonium chloride and substitution with glycine betaine were the most frequent methods adopted; the main disadvantage of the latter was the need for organic solvents, while, in the former, the reaction was conducted in water media.[26] In addition, the use of choline chloride has been reported to obtain water-soluble cationic cyclodextrin-based polymers. In this case, choline chloride was added as a functional cationic molecule together with

Department of Chemistry, NIS Centre, University of Turin, Via P. Giuria 7, 10125 Torino, Italy. E-mail: claudio.cecone@unito.it

the monomer and cross-linker during the synthetic step, to add to the final product positive amino functions.[36] Generally speaking, bio-based materials are considered to be more sustainable than conventional petrochemical ones, as they are obtained from renewable rather than non-renewable raw materials.[37] In this context, maltodextrins are defined as water-soluble starch hydrolysis products, which are used mostly as food and pharmaceutical additives.[38] They are considered to be D-glucose polymers, characterised by α-(1,4) and α-(1,6) glycosidic linkages, thus composed of amylose and amylopectin degradation products.[39] In their definition, maltodextrins are characterised by a dextrose equivalent (DE) <20, a value representing the reducing equivalence of a given carbohydrate against the same mass of glucose.[40] Nevertheless, their hydrophilic features and good water solubility has limited their use in those applications where cross-linked polymers with certain mechanical properties were required. For this reason, there have been numerous attempts to cross-link soluble polysaccharides exploiting suitable cross-linkers such as epichlorohydrin, isocyanates, poly-amines, carbodiimide, glutaraldehyde, and poly-carboxylic acids.[41–47] Among the aforementioned cross-linkers, water-soluble diglycidyl ethers have been reported to be useful functional molecules for achieving grafting and hydrogels formation from hyaluronic acid, chitosan, and β-cyclodextrin molecules.[48–54] Furthermore, 1,4-butanediol diglycidyl ether has revealed excellent non-toxic and biocompatible features;[55] for this reason, it has been applied in many studies concerning the loading-release of drugs.[48] Having said this, with the aim of producing water-insoluble carbohydrate-based polymers suitable for sustainable scaling-up, in awareness of the pivotal role of amines in epoxy-based polymer production, amine-mediated ring-opening reaction of diglycidyl ether was exploited to cross-link suitable water-soluble maltodextrins, using water as a unique solvent and green reactants only. In this work, a commercial maize-derived maltodextrin (Glucidex 2®) was used as a building-block, 1,4-butanediol diglycidyl ether as a cross-linker, while 1,4-diazabicyclo[2.2.2]octane, imidazole, triethylamine, and guanidine hydrochloride were used to obtain the amine-mediated epoxy ring-opening reaction.

Experimental

Materials

Glucidex 2® (GLU2) was provided by Roquette Freres (Lestrem, France), while 1,4-diazabicyclo[2.2.2]octane (DABCO), imidazole (IMI), triethylamine (TEA), guanidine hydrochloride (GUA), and 1,4-butanediol diglycidyl ether (BDE) were purchased from Sigma-Aldrich (Darmstadt, Germany). GLU2 was dried in an oven at 75 °C up to constant weight before use.

Polymer synthesis

In a typical procedure, the synthesis of the polymer was carried out by dissolving 1.75 g of GLU2 in 5 mL of 0.2 M NaOH sodium hydroxide distilled water solution, using a round-bottom flask. Thereafter, while continuously stirring the solution, the amine (DABCO, IMI, TEA, GUA) was added at a certain molar ratio (1 : 2, 1 : 4, and 1 : 8 mol : mol) in respect of BDE, as reported in Table 1. Then, 0.35 mL of BDE was added, and the temperature was increased to 70 °C, using a hotplate stirrer equipped with thermoregulation and a metal hemispheric bowl to obtain homogeneous heating of the flask. The reaction was then allowed to occur for 90 minutes, ultimately obtaining a monolith block as the product. Later, the product was recovered from the flask by crushing with a spatula and subsequently purified with distilled water to remove any non-reacted reagents. At the end of the purification step, the product was dried in an oven at 70 °C up to constant weight and grinded with a mortar, obtaining a powder. The amount of polymer resulting after purification was described as mass balance and consisted of roughly 70 to 85% of the initial weight (Fig. 1). All these details are discussed in the results and discussion section. To obtain information on reproducibility, all reported syntheses (Table 1) were performed in triplicate, thus all results will be expressed as mean value.

Table 1 Syntheses performed

Amine	Amine : BDE mol : mol ratio (%)/sample name		
BLANK	0 (synthesis without amine)/N		
DABCO	12.5 (27 mg)/D_12.5	25 (54 mg)/D_25	50 (108 mg)/D_50
IMI	12.5 (16 mg)/I_12.5	25 (33 mg)/I_25	50 (66 mg)/I_50
TEA	12.5 (24 mg)/T_12.5	25 (49 mg)/T_25	50 (98 mg)/T_50
GUA	12.5 (14 mg)/G_12.5	25 (28 mg)/G_25	50 (57 mg)/G_50

TGA characterization

Thermogravimetric analyses (TGA) were carried out using TA Instruments Q500 TGA (New Castle, DE, USA), from 50 °C to 700 °C, under nitrogen flow, with a heating rate of 10 °C min^{-1}.

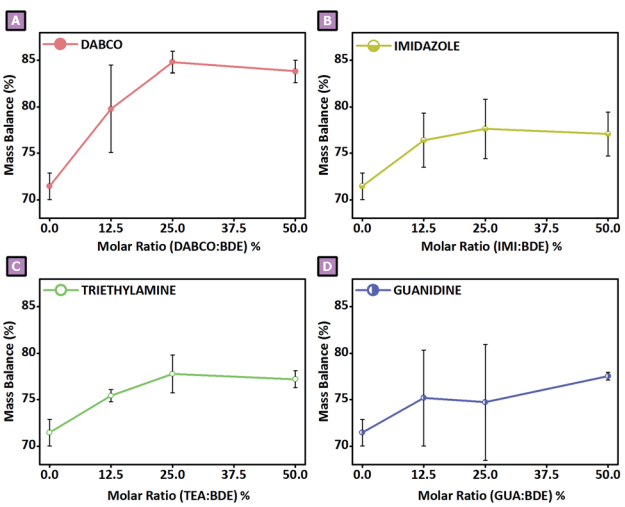

Fig. 1 Mass balance in function of (A) DABCO : BDE, (B) IMI : BDE, (C) TEA : BDE, and (D) GUA : BDE molar ratio.

FTIR-ATR analysis

A PerkinElmer Spectrum 100 FT-IR Spectrometer (Waltham, MA, USA) equipped with a Universal ATR Sampling Accessory was used for FTIR-ATR (Attenuated Total Reflection) characterisation. All spectra were collected in the wavenumber range of 650–4000 cm^{-1}, at room temperature, with a resolution of 4 cm^{-1} and 8 scans per spectrum.

Elemental analysis characterization

The samples chemical composition was studied using a Thermo Fisher FlashEA 1112 Series elemental analyser (Waltham, MA, USA).

NMR characterization

All H^1 NMR spectra were obtained using a Bruker AVANCE 200 MHz spectrometer (Bruker, MA, USA), with D_2O as solvent. The concentration of reagents in D_2O was approximately 10 wt%.

Swelling tests

The swelling tests were performed by adding to 10 mL of distilled water 200 mg of polymer obtained from each synthetic condition. The samples were subsequently allowed to swell for 24 hours. After the removal of the liquid phase *via* centrifugation, the swelling percentage was calculated as follows:

$$\%\ \text{swelling} = \left(\frac{g_{(\text{swelled polymer})} - g_{(\text{dry polymer})}}{g_{(\text{dry polymer})}} \right) \times 100 \quad (1)$$

ζ-Potential analysis

A Malvern Zetasizer Nano – ZS (Malvern, United Kingdom) was used to measure the zeta potential. All the tests were performed using distilled water at room temperature.

SEM characterization

The morphology of the samples was studied using scanning electron microscopy (SEM). The images were acquired with a Zeiss EVO 50 (Oberkochen, Germany) using secondary electrons and 10 kV accelerating voltage. Prior to SEM characterisation, the samples were ion-coated with gold using a Baltec SCD 050 sputter coater (Pfäffikon, Switzerland) for 40 seconds, under vacuum, at 60 mA.

Gas-volumetric analysis

Nitrogen adsorption–desorption isotherms were measured at 77 K using a Micromeritics ASAP2010 volumetric sorption analyzer (Norcross, GA, USA). Prior to the adsorption measurements, the sample was outgassed at 100 °C under vacuum (10 mm Hg) for 15 hours to remove the adsorbates and residual moisture. The specific surface area was estimated using the BET equation.

Probe molecules adsorption tests

Probe molecule adsorption tests were performed starting from 10 mL of a 1, 5, 10, 25, 50, and 100 mg L^{-1} Orange II sodium salt distilled water solution, at room temperature. The adsorption test for each concentration was performed in triplicate by preparing a 10 mg D_50 dispersion in the probe solution. All the dispersions were continuously stirred at room temperature, then UV-vis spectra were acquired (Orange II λ_{max}: 486 nm) using a PerkinElmer Lambda 25 UV/vis spectrometer (Waltham, MA, USA), after 15 hours. A centrifuge was used to separate the polymer from the solution before UV-vis measurement.

Results and discussion

Material design and characterization

BDE has been extensively reported to react as a linker agent even in mild reactive conditions. The ring-opening reaction was reported to occur in water media already at 50 °C in base-catalysed conditions, without involving the formation of any charged functions.[54] On the other hand, as previously described, with the aim of observing the effects of adding amines to the reported systems, amine-mediated ring-opening reactions of BDE were studied to cross-link a commercial water-soluble maltodextrin (Glucidex 2®). As a result, the presence of peculiar surface charges characterising the final products were observed, a feature that enabled us to hypothesise the presence of a specific reactive path involving the amine introduced as catalyst. Therefore, to shed light on what we observed, the reported synthetic approach and the resulting products were extensively studied and discussed. An initial comparison was performed by observing the amount of product recovered from each synthetic condition. The amount of polymer obtained after the purification and drying process was expressed as the mass balance, considering the weight of the final product with respect to the theoretical weight, equal to the sum of GLU2, BDE, and the amine when present, as reported in Fig. 1. The mass balance ranged roughly from 70% to 85%. With regard to sample N, the presence of the amine increased the mass balance in all cases (Fig. 1). The higher value was observed for sample D_25 (Fig. 1A) and was 84.8%, whereas the lower value, as anticipated, was observed for sample N and was 71.4%. Except for guanidine-mediated reactions (Fig. 1D), in the other cases a similar trend was observed, consisting of the presence of a maximum centred at amine : BDE mol : mol ratio of 25%, followed by a slight decrease in the mean mass balance, for higher amounts of amine. The obtained polymer samples were later morphologically characterised; the presence of transparent dimensionally polydispersed polymer granules could be observed (Fig. 2), whose size was roughly between a few tens to one hundred microns. The presence of amine-mediated reactions led to polymers characterised by increasing yellowing, proportional to the increasing amount of amine, when compared to the results observed from sample N. This feature was found to be more pronounced in DABCO, IMI, and TEA-mediated products. The SEM characterisation (Fig. 2) revealed smooth external surfaces and the absence of macro-porosity. The porosity was further studied by gas-volumetric analysis, which confirmed the bulky features of the resulting polymer granules. The specific surface areas were comprised roughly between 1 and 2 $m^2\ g^{-1}$, while the absence of any meso- and

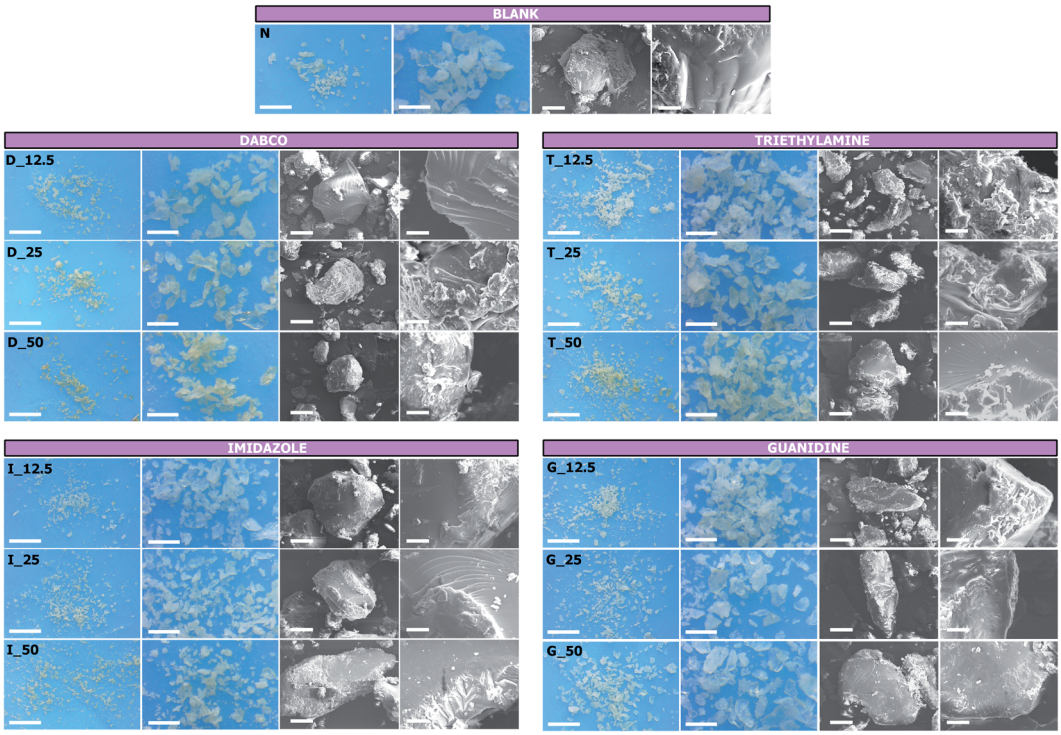

Fig. 2 Polymer granules and SEM images of the polymer products obtained from each synthetic condition. Scale bars: 1 mm (first column); 250 μm (second column); 50 μm (third column); 10 μm (fourth column).

micro-porosity was also observed. Subsequently, the thermal stability of each product was studied *via* thermogravimetric analysis. TGA were carried out and the related onset temperatures (T_{onset}) are reported in Table 2. All samples described a similar TGA profile; for this reason, only the thermogram related to sample N is reported in Fig. 3, for descriptive clarity. As reported in Fig. 3, the TGA was characterised by two main weight loss phenomena: the initial one occurred between approximately 50 °C and 150 °C and related to the volatilisation of the water adsorbed on the surface of the sample and amounted to 6.3 ± 1.1% of the initial weight. Subsequently, a second weight loss phenomenon was observed between 250 °C and 450 °C which was related to the pyrolysis of the system, giving a carbon residue corresponding to 13.4 ± 1.9% of the initial weight; the latter was found to be stable up to 700 °C. As noted, the second weight loss phenomenon, which was related to degradative reactive paths, was used to obtain *via* graphical elaboration of the curve the T_{onset}, and was then associated with the thermal stability of the sample. Table 2 reveals how the presence of amine-mediated reactions could be associated with a decrease in the thermal stability of the resulting polymer. Moreover, the decrease in thermal stability was dependent on the amount of amine introduced. A thermal stability decrease of 1.3 ± 2.1% could be calculated for amine : BDE mol : mol ratio of 12.5%, a decrease of 2.4 ± 1.8% for amine : BDE mol : mol ratio of 25%, and finally a decrease of 4.0 ± 1.9% for amine : BDE mol : mol ratio of 50%. Furthermore, an important feature concerning cross-linked polymers consists of the swelling properties displayed towards solvents and water, particularly in terms of bio-based systems. For this reason, in spite of the non-porous features observed from the gas-volumetric analysis and morphological characterisation,

Table 2 T_{onset} resulting from TGA

Sample	T_{onset} (°C)	Sample	T_{onset} (°C)
N	318	I_12.5	321
D_12.5	314	I_25	311
D_25	310	I_50	317
D_50	300	G_12.5	315
T_12.5	305	G_25	311
T_25	303	G_50	310
T_50	300		

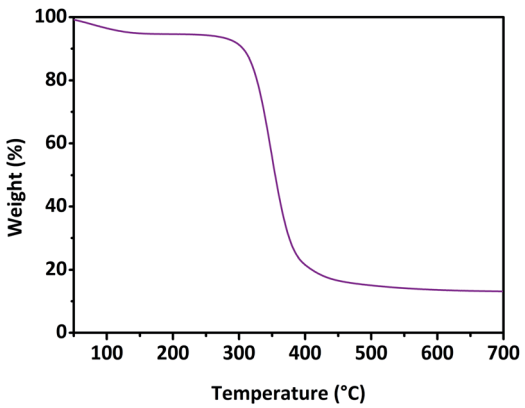

Fig. 3 TGA of sample N.

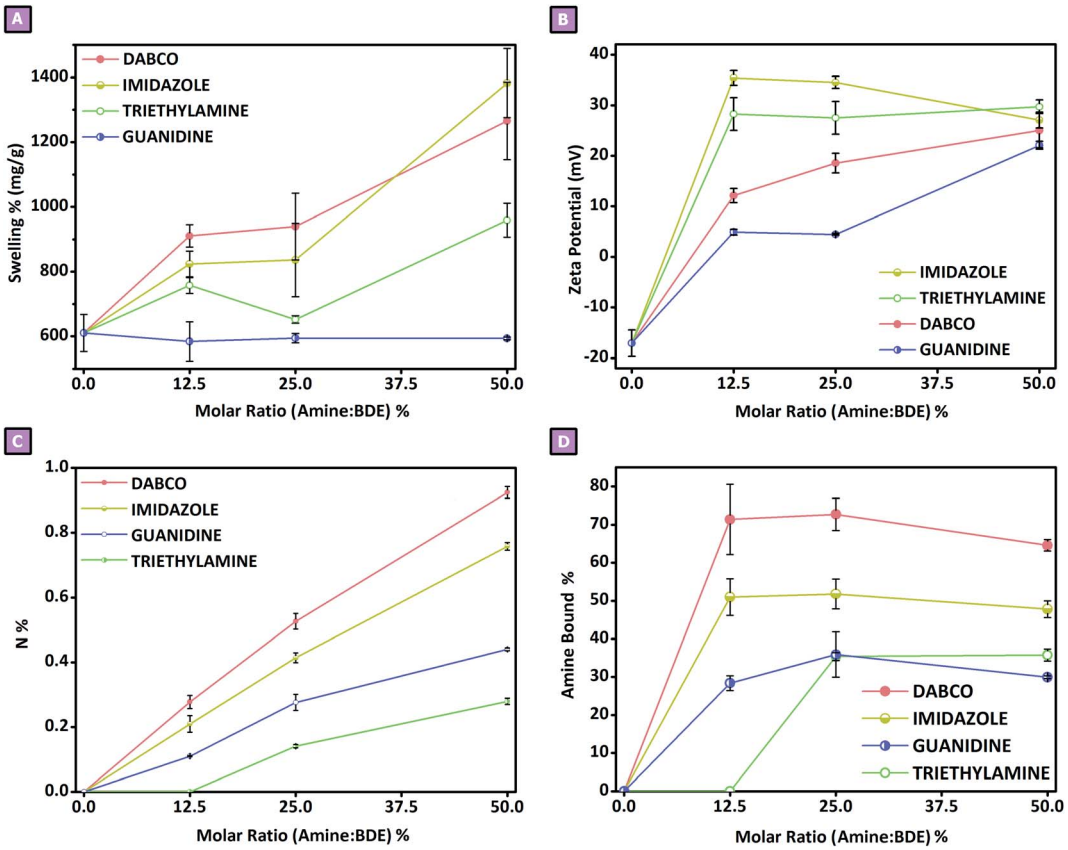

Fig. 4 Swelling% (A), zeta potential (B), elemental analysis (C) and amine bound% (D) based upon each amine : BDE molar ratio.

swelling tests were performed on each product obtained. Despite the capability of these polymers to display a certain affinity also towards organic polar solvents, the focus has been put on using distilled water at room temperature, to evaluate the possibility of further studies for environmental, pharmaceutical or medical applications; the results obtained, expressed as the swelling percentage, are reported in Fig. 4A. As shown in Fig. 4A, the obtained swelling values ranged roughly from 600% to 1400%. The systems affected more strongly by the presence of amine-mediated reactions were DABCO-mediated and IMI-mediated synthesis, followed by TEA-mediated reaction products; the presence of GUA-mediated reaction did non display any change to the swelling feature of the system. In the case of DABCO-mediated and IMI-mediated syntheses, the products displayed higher swelling properties, in which the increase in swelling values was proportional to the increase in the amine : BDE mol : mol ratio. Sample N displayed a swelling value of 610 ± 57%, whereas the highest values were observed for samples I_50 and D_50 which amounted to 1383 ± 107% and 1266 ± 120%, respectively. TEA-mediated syntheses displayed a lower increase in swelling values compared to the systems described above; nevertheless, sample T_50 revealed a swelling of 959 ± 52%. From this first characterisation step, it was clear to see how the amine-mediated reactions had an influence on the resulting polymer product. For this reason, to obtain a better understanding of the role of amine in the polymerisation reaction, the ζ-potential displayed by each product was also studied. All tests were carried out in distilled water at room temperature. As reported in Fig. 4B, only sample N displayed a negative ζ-potential, probably due to the presence of many hydroxy functions. On the contrary, all samples obtained *via* amine-mediated reactions displayed positive ζ-potential values caused by the presence of positive charges within the polymer structure. To shed light on this result, elemental analyses were performed for all synthesised samples. As reported in Fig. 4C, in the presence of amine-mediated reactions, a nitrogen content was detected within the sample, while its absence was observed for sample N. The nitrogen amount ranged from approximately 0.10 wt% to 1.00 wt%. The lower value was observed for sample T_12.5; in this case, the amount of nitrogen, which was negligible, was probably too low to be detected *via* elemental analysis. Conversely, in the case of D_50, a nitrogen content of 0.92 wt% was detected and corresponded to the higher value obtained. For all systems studied, a positive trend was observed when increasing the amount of amine: the higher the amount of amine used to obtain amine-mediated reactions, the greater the nitrogen content detected. From what we observed, as the amines were the only reactants carrying nitrogen atoms, in the knowledge that the product was purified after synthesis, we were able to hypothesise that the amines could be chemically bound to the polymer structure, and thus might have an active role during polymerisation. Having said that, according to the proposed mechanisms reported for the amine-mediated ring-opening reaction, two distinct phases could be hypothesised

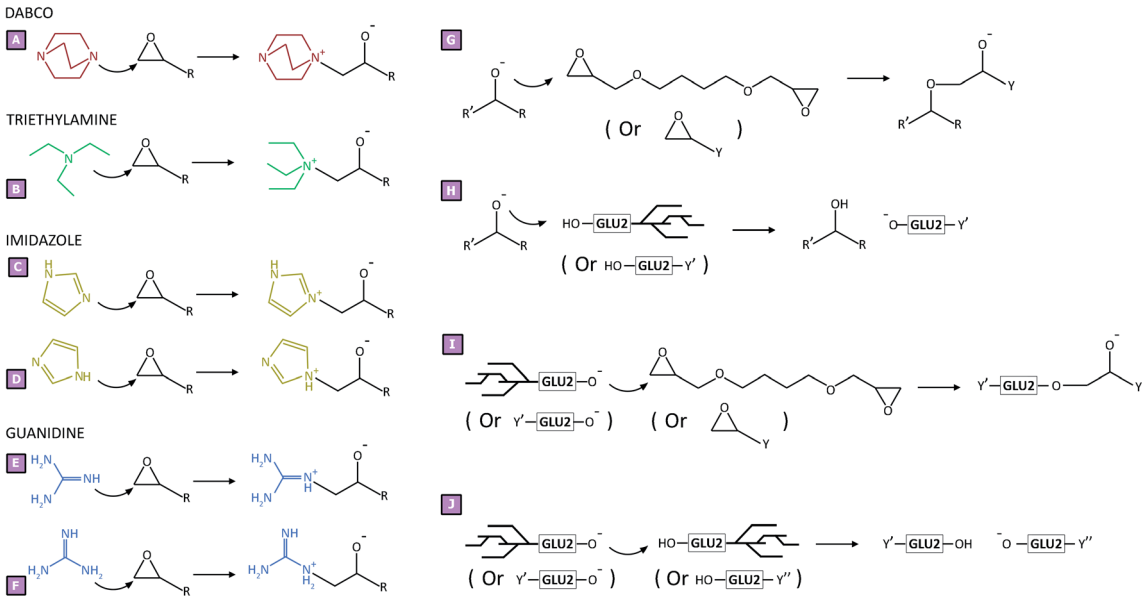

Fig. 5 Amine-mediated ring-opening reactions of BDE (A–F). Chain growth reactions by alkoxides species reacting with BDE molecules and GLU2 molecules (G–J).

which characterised the generation of the polymer network.[13,14,21–23] An initial interaction (Fig. 5A–F), occurring between the chosen amines and the linker, was hypothesised to generate reactive species which subsequently led to the actual growth of polymer chains (Fig. 5G–J), characterising the second phase. As reported in Fig. 5A–F, the generation of quaternary ammonium functions was hypothesised as the initial product. Moreover, due to the high pH value characterising the synthetic conditions, the presence of alkoxides functions was also expected, as a result of the ring-opening. This initial step might facilitate the production of reactive alkoxides acting as precursor-like species, which could initiate the subsequent polymerisation step (Fig. 5G–J). The contents of Fig. 5A–F were supported by H^1 NMR spectra carried out in D_2O on reaction products obtained by reacting each amine with BDE in distilled water at 70 °C for 30 minutes. The chemical shifts observed (Fig. 6) after the interaction of each amine with BDE were initial evidence of the actual presence of amine-mediated ring-opening reaction products. Furthermore, the absence of typical epoxy proton resonance at 2.7, 2.9, and 3.3 ppm (Fig. 6G–K), which disappeared upon reaction with the tested amines, also allowed us to confirm the hypothesised mechanism. Once formed, as the alkoxides are highly reactive species, they could display some reactivity towards either other epoxide rings belonging to BDE molecules or hydroxyl functions from GLU2 (Fig. 5G–J). In the first case, the result could be associated with a propagation of the alkoxide species, but a negligible molecular weight increase, if associated with unreacted BDE molecules (Fig. 5G). On the other hand, a proton transfer from a GLU2 chain to the previously generated alkoxide might lead to the formation of alkoxide functions along the GLU2 backbone (Fig. 5H and J). The alkoxides generated on the backbone of GLU2 molecules could further react with other epoxides rings, being present either as free BDE molecules or terminal reactive functions of growing macromolecule chains (Fig. 5I). In the awareness that GLU2 is characterised by a molecular weight of approximately 300 kDa,[56] the chain growth given by this latter reactive path was hypothesised to be of great impact. The alkoxides present along the GLU2 backbone might also have reacted with other GLU2 molecules describing a transfer of the alkoxide function *via* proton transfer reaction, thereby generating new alkoxide species. Eventually, the generation of a cross-linked network has been hypothesised to be the result of the aforementioned reactive paths. The hypothesised reaction mechanisms did not differ from a standard base-catalysed reaction; nevertheless, the higher nucleophilicity displayed by amines when compared to hydroxide revealed that the reported paths were likely to be kinetically favoured. Taking into account what is hypothesised above, some considerations could be made regarding the observed results. In relation to the mass balance, the presence of a maximum centred at amine : BDE mol : mol ratio of 25%, followed by a slight decrease in the mean value for higher amounts of amine, was observed (Fig. 1). This behaviour might be related to the excessive number of epoxy rings involved in the amine-mediated ring-opening step, resulting in a depletion of BDE molecules suitable to react as liker between two growing polymer chains; for this reason, low molecular weight branched water-soluble segments might have been removed as a by-product during the purification step. Furthermore, by assuming that all amine amounts introduced during the synthesis ended up in the polymer network, and comparing it with the nitrogen content obtained *via* elemental analysis, normalised by the number of nitrogen atoms composing the chosen amine, we could calculate the actual fraction of amine present in the final product compared with the theoretical 100% value. Fig. 4D revealed that DABCO was the amine retained in the higher quantity, followed by IMI, and finally by GUA and TEA. The highest value was observed for

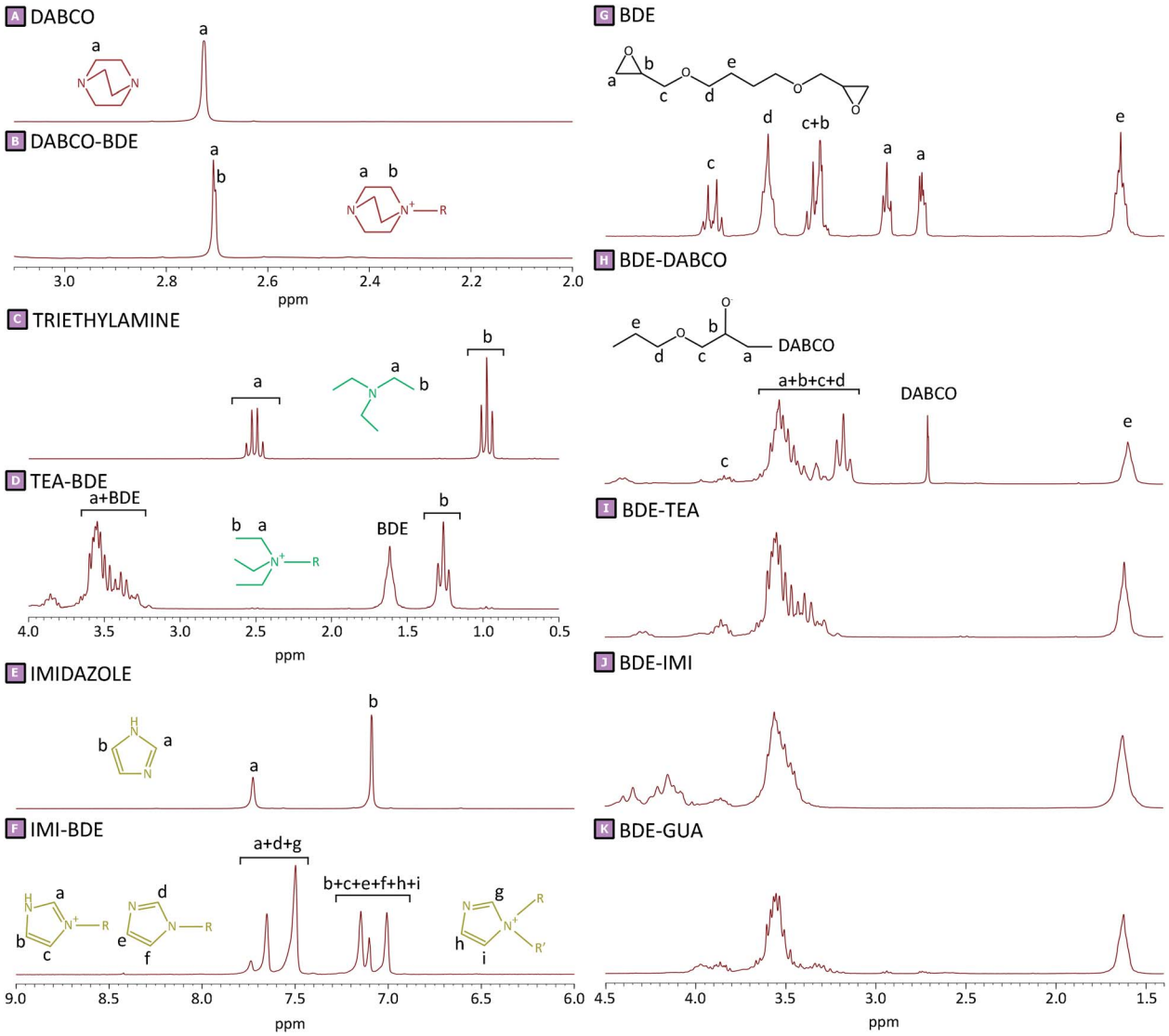

Fig. 6 H^1 NMR spectra of DABCO, TEA, and IMI before and after reaction with BDE (A–F). H^1 NMR spectra of BDE before and after reaction with DABCO, TEA, IMI, and GUA (G–K).

sample D_25 and amounted to 72.7%; the highest value for IMI-mediated syntheses was 51.8% (I_25), while for TEA-mediated and GUA-mediated syntheses, it was 35.8% (T_50) and 35.9% (G_25), respectively. Generally speaking, as observed in the results related to mass balance, also in this case a trend characterised by a maximum centred at amine : BDE mol : mol ratio of 25% could be identified. This behaviour could be justified, as in the case of mass balance, by the effects brought on by the amine; in this case, the presence of a large quantity of amine might result in BDE molecules double bonded with two amine molecules and thus less prone to becoming part of the polymer network. Therefore, as the latter are present as by-products, they might have been separated from the product during the purification step resulting in a depletion of the amine present in the purified samples. Furthermore, the mechanism hypothesised to be behind the different behaviour displayed by each amine is closely connected with what is described above. As mentioned, the number of amines bound to the polymer network differed from one amine to the other; DABCO displayed the highest efficacy on being retained in the final product, followed by IMI, and finally by TEA and GUA. An initial reason for this may relate to differences in the nucleophilicity of the amine; that said, tertiary amines should have been more favoured than primary and secondary amines. However, although TEA is a tertiary amine, it might be affected by the presence of ethyl pendants surrounding the nitrogen atom, which might have hindered the attack to the epoxy ring. A second explanation might relate to the presence of intramolecular hydrogen transfer taking place as soon as the epoxy ring underwent ring-opening reaction; following this path the alkoxide species generated as a consequence of the epoxy opening might have been protonated *via* proton transfer from the amine functions, de-activating the reactivity previously hypothesised for the alkoxide species (Fig. 5). Therefore, as GUA is characterised by primary amine groups, it might have been deeply affected by this phenomenon, resulting in a low retention to the final product. Considering

these aspects, the results experimentally obtained fit in with the hypothesised mechanism; DABCO, being a cyclic molecule with only tertiary amines, could not be affected by either of the aforementioned phenomena. IMI, displaying a hydrogen bound to one of its two nitrogen atoms, might have suffered from the presence of intramolecular proton transfer following the epoxy opening, determining a lower amount of amine in the final product when compared to DABCO-mediated syntheses. Furthermore, the presence of intramolecular proton transfer phenomena might also have affected the formation of quaternary ammonium functions. For this reason, a spectroscopic investigation was carried out on the products obtained. As reported in Fig. 7, the presence of quaternary ammonium groups was studied in the spectroscopic range between 1500 cm^{-1} and 1750 cm^{-1}; mainly DABCO-mediated (Fig. 7A) and IMI-mediated (Fig. 7B) reactions displayed the presence of signals in that spectral region. In the first case, due to the absence of hydrogen atoms which could lead to proton transfer from the amine to the alkoxide, the presence of quaternary ammonium was confirmed, observing a peak centred at 1590 cm^{-1}. The intensity of the signal also appeared to be directly dependent on the amine : BDE mol : mol ratio, in further confirmation. Similarly, but less intensely, IMI-mediated reactions also displayed a peak centred at 1590 cm^{-1}; however, in this second case, the presence of a shoulder centred at 1567 cm^{-1} suggested the presence of quaternary ammonium atoms characterised by different chemical surroundings. This observation may be related to the possibility of IMI attacking the epoxy ring through both the nitrogen atoms displayed by its structure, as shown in Fig. 5. The very low signals displayed by TEA-mediated reaction products (Fig. 7C) were further confirmation of the low efficacy of TEA in the ring-opening reaction of BDE's epoxy rings, as previously suggested by the elemental analysis results and the subsequent calculations related to the amount of amine present in the final product. Ultimately, the presence of any signals in the GUA-mediated syntheses (Fig. 7D) was evidence that all ring opening reactions occurring *via* the amine-mediated mechanism resulted in a proton transfer. However, if all the proton transfer occurred from the amine associated with the nucleophilic attack, changes in the mass balance would be observed when changing the amine : BDE mol : mol ratio. In addition, if all the proton transfer occurred from the amine associated with the nucleophilic attack, a depletion of BDE molecule suitable to cross-link the growing polymer chains would be expected, resulting in a decrease in the mass balance value instead (Fig. 1). As none of these aspects were observed in the related systems, we were able to hypothesise that a fraction of the proton transfer did not occur from the amine but rather from the deprotonation of GLU2 hydroxyl groups. Moreover, it was not possible to exclude also a further attack of the alkoxide obtained through amine-mediation towards another BDE's epoxy ring before the proton transfer occurred, allowing for a propagation of the alkoxide species. What was hypothesised for GUA-mediated reactions could also be extended to the other amine-mediated polymerisation and considered, together with the reactions reported in Fig. 5, as reactive paths taking place during the formation of the polymer network. Similarly, the increasing of the swelling features (Fig. 4A) observed upon amine-mediated syntheses could be related firstly to all the BDE molecules bound to an amine rather than acting as a bridge between two GLU2 molecules. This feature might lead to a less compact network which could display higher mobility of the polymer segments composing the polymer structure, resulting in increased absorbing features. Further, the presence of amino pendants could result in more hydrophilic polymer networks, capable of absorbing and retaining higher quantities of water. In addition, the inefficacy displayed by GUA-mediated reactions could be due to the low amount of GUA retained in the final product and to the fact that none of the mediated ring-openings occurred with the formation of a quaternary ammonium, as suggested by the FTIR-ATR results. This feature might have hindered the formation of wider polymer networks due to the absence of electrostatic repulsion phenomena. Ultimately, the positive values obtained from the ζ-potential analyses could be due to the presence of either quaternary ammonium functions (DABCO, IMI, TEA) or protonated amino pendants (IMI, GUA), in further confirmation of the reactive paths previously proposed.

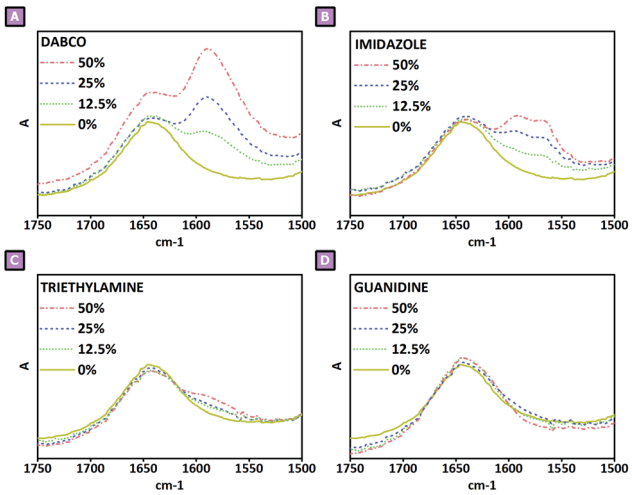

Fig. 7 FTIR-ATR spectra of amine-mediated synthesis products, obtained from (A) DABCO, (B) IMI, (C) TEA, and (D) GUA.

Evaluation of adsorption performances

Additional information on the adsorption capacity of the cross-linked polymer was obtained through adsorption tests carried out on water solutions of Orange II (OR). Considering that OR is negatively charged, electrostatic interaction towards the polymer sample was expected. Polymer suspensions were prepared at increasing concentration of the probe molecule, and the UV-vis adsorptions were collected after 15 hours. The percentage of probe molecule adsorbed by the polymer in respect of the starting concentration (% absorbed) was calculated as:

$$\%\ \text{adsorbed} = \left(1 - \frac{\text{Conc}\ \ t_{(x)}}{\text{Conc}\ \ t_{(0)}}\right) \times 100 \qquad (2)$$

where, Conc $t_{(x)}$ represents the concentration in mg L^{-1} of probe molecule at $t_{(x)}$ (with x equal to 15 hours) and Conc $t_{(0)}$ the

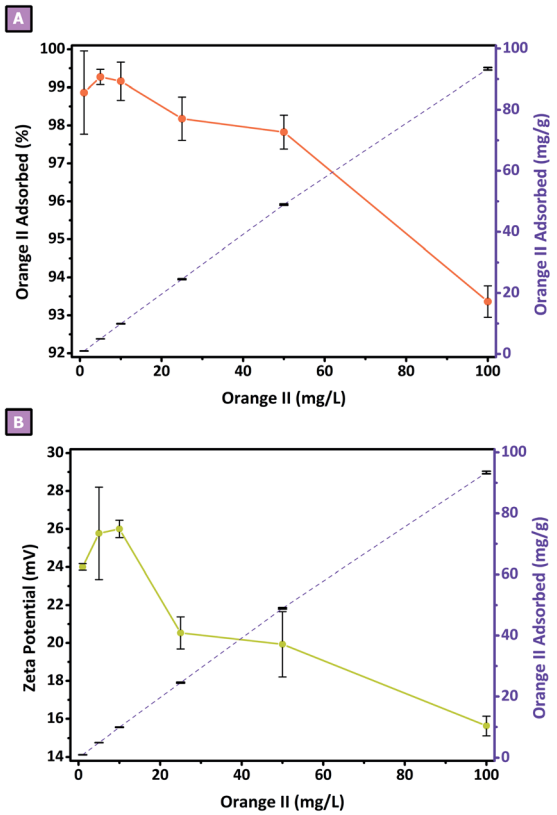

Fig. 8 Adsorption tests of Orange II. (A) % adsorbed *vs.* Conc. $t_{(0)}$. (B) Zeta potential *vs.* Conc. $t_{(0)}$.

concentration in mg L^{-1} of probe molecule at t_0 (equal to 1, 5, 10, 25, 50, and 100 mg L^{-1}). The % absorbed *vs.* Conc $t_{(0)}$ is reported in Fig. 8A. After 15 hours the % adsorbed from all the Conc $t_{(0)}$ tested was higher than 90%. From Conc $t_{(0)}$ of 1, 5, and 10 mg L^{-1}, the % adsorbed was almost total (98.9 ± 1.1, 99.2 ± 0.2, and 99.2 ± 0.5%, respectively) while from 25 to 100 mg L^{-1} a decrease was observed. The lower % adsorbed was observed from 100 mg L^{-1} OR solution and amounted to roughly 93%. Moreover, when considering the adsorption of OR in terms of $mg_{(Orange\ II)}\ g_{(polymer)}^{-1}$ a proportional increase in respect to the Conc $t_{(0)}$ was observed (Fig. 8); the higher adsorption was observed from 100 mg L^{-1} OR solution and was 93.4 ± 0.4 mg g^{-1}. In addition, to demonstrate the presence of electrostatic interaction, the ζ-potential of each suspension was measured, after the 15 hours adsorption test. As reported in Fig. 8B, a decrease in the ζ-potential values, proportional to the increasing Conc $t_{(0)}$ was obtained, as evidence of what is hypothesised above. Conc $t_{(0)}$ of 1, 5, and 10 mg L^{-1} did not affect the ζ-potential of the pristine polymer, which was 25.0 ± 3.5 mV, while from 25 mg L^{-1} a proportional decrease was observed. The lower value resulted from 100 mg L^{-1} OR solution, equal to 15.6 ± 0.85 mV.

Conclusions

The diglycidyl ether epoxy ring-opening reaction by amine was proven to be a suitable approach for achieving the cross-linking of maltodextrins. It has been demonstrated that it is possible to obtain a one-step synthesis of positive-charged water-insoluble bio-based polymer networks without using additional charged molecules. Moreover, this approach avoided the use of any organic solvent by performing the synthesis in water media. Glucidex 2®, a suitable maize-derived maltodextrin, was used as building-block, while 1,4-butanediol diglycidyl ether (BDE) was chosen as cross-linker thanks to its good water solubility, low toxicity, and biocompatibility. 1,4-Diazabicyclo[2.2.2]octane (DABCO), imidazole (IMI), triethylamine (TEA), and guanidine hydrochloride (GUA) were tested to obtain the amine-mediated ring opening reaction of BDE's epoxide rings, at different amine : BDE mol : mol ratios of 12.5%, 25% and 50%. All studied synthetic conditions allowed us to obtain a polymer product; its mass balance was higher in the presence of amine-mediated reactions than in base-catalysed conditions only, and was dependent on the amount of amine added during the synthesis. The fraction of amine retained in the final product was studied *via* elemental analysis and was found to be affected by the nucleophilicity of each amine and by the presence of proton transfer reactions occurring from the amine responsible for the nucleophile attack and alkoxide resulting from the epoxy ring-opening. Furthermore, in the case of tertiary amines, the ring-opening reaction resulted in the formation of ammonium species, as confirmed by FTIR-ATR characterisation; also in this case, the latter was found to depend upon the amine : BDE mol : mol ratio. In addition, the swelling features towards water were increased by the presence of amine-mediated reaction which allowed polymers to be obtained characterised by lower cross-linking density and more hydrophilic features. Further, the presence of positive charges on each product water suspension was confirmed, due to the presence of the aforementioned quaternary ammonium functions or protonated amines. Eventually, high adsorbing features were observed from probe molecule adsorption tests, carried out in water at room temperature. In this work, we have been able to demonstrate how the combination of maltodextrins, diglycidyl ethers and amines is a useful and sustainable approach for obtaining one-step syntheses of cationic bio-based polymers suitable for eco-friendly scaling-up, while the high adsorbing feature displayed allows these materials to be further studied as green adsorbents for environmental, pharmaceutical and medical applications.

Author contributions

Claudio Cecone: conceptualization, methodology, investigation, validation, formal analysis, visualization, writing – original draft, writing – review & editing. Giulia Costamagna: methodology, investigation, validation, writing – review & editing. Marco Ginepro: supervision, methodology, writing – review & editing. Francesco Trotta: supervision, project administration, writing – review & editing.

Conflicts of interest

There are no conflicts to declare.

References

1 R. Auvergne, S. Caillol, G. David, B. Boutevin and J. P. Pascault, *Chem. Rev.*, 2014, **114**, 1082–1115.
2 F. L. Jin, X. Li and S. J. Park, *J. Ind. Eng. Chem.*, 2015, **29**, 1–11.
3 L. N. Vandenberg, R. Hauser, M. Marcus, N. Olea and W. V. Welshons, *Reprod. Toxicol.*, 2007, **24**, 139–177.
4 E. R. Rad, H. Vahabi, A. R. de Anda, M. R. Saeb and S. Thomas, *Prog. Org. Coat.*, 2019, **135**, 608–612.
5 P. T. Anastas and M. M. Kirchhoff, *Acc. Chem. Res.*, 2002, **35**, 686–694.
6 P. T. Anastas and N. Eghbali, *Chem. Soc. Rev.*, 2010, **39**, 301–312.
7 M. Chrysanthos, J. Galy and J. P. Pascault, *Polymer*, 2011, **52**, 3611–3620.
8 C. Aouf, H. Nouailhas, M. Fache, S. Caillol, B. Boutevin and H. Fulcrand, *Eur. Polym. J.*, 2013, **49**, 1185–1195.
9 J. M. Raquez, M. Deléglise, M. F. Lacrampe and P. Krawczak, *Prog. Polym. Sci.*, 2010, **35**, 487–509.
10 J. H. Hodgkin, G. P. Simon and R. J. Varley, *Polym. Adv. Technol.*, 1998, **9**, 3–10.
11 V. F. Stroganov, *Polym. Sci.*, 2014, **7**, 73–76.
12 M. Inoki, S. Kimura, N. Daicho, Y. Kasashima, F. Akutsu and K. Marushima, *J. Macromol. Sci., Part A: Pure Appl. Chem.*, 2002, **39**(4), 321–331.
13 F. López-barajas, L. F. Ramos-devalle, S. Sánchez-valdes and E. Ramírez-vargas, *Polym. Test.*, 2019, **73**, 346–351.
14 W. R. Ashcroft, in *Chemistry and Technology of Epoxy Resins*, 1993, pp. 37–71.
15 G. Sun, J. Liu, X. Wang, M. Li, X. Cui, L. Zhang, D. Wu and P. Tang, *Eur. Polym. J.*, 2019, **114**, 338–345.
16 J. Hong and A. Khan, *Polymers*, 2019, **11**, 1941.
17 H. C. Kolb, M. G. Finn and K. B. Sharpless, *Angew. Chem., Int. Ed.*, 2001, **40**, 2004–2021.
18 S. J. Stropoli and M. J. Elrod, *J. Phys. Chem. A*, 2015, **119**, 10181–10189.
19 N. Cengiz, *Eur. Polym. J.*, 2020, **123**, 109441.
20 Y. I. Estrin, A. E. Tarasov, A. A. Grishchuk, A. V. Chernyak and E. R. Badamshina, *RSC Adv.*, 2016, **6**, 106064–106073.
21 J. Oh, K. I. Jung, H. W. Jung and A. Khan, *Polymers*, 2019, **11**, 1491.
22 J. Wu and H. G. Xia, *Green Chem.*, 2005, **7**, 708–710.
23 A. Saha, S. De, M. C. Stuparu and A. Khan, *J. Am. Chem. Soc.*, 2012, **134**, 17291–17297.
24 Y. Yu, M. Shen, Q. Song and J. Xie, *Carbohydr. Polym.*, 2018, **183**, 91–101.
25 X. Qi, L. Wu, T. Su, J. Zhang and W. Dong, *Colloids Surf., B*, 2018, **170**, 364–372.
26 H. J. Prado and M. C. Matulewicz, *Eur. Polym. J.*, 2014, **52**, 53–75.
27 M. R. Kweon, F. W. Sosulski and P. R. Bhirud, *Starch/Staerke*, 1997, **49**, 59–66.
28 R. S. Blackburn, *Environ. Sci. Technol.*, 2004, **38**, 4905–4909.
29 A. Mignon, N. De Belie, P. Dubruel and S. Van Vlierberghe, *Eur. Polym. J.*, 2019, **117**, 165–178.
30 J. Desbrières and E. Guibal, *Polym. Int.*, 2018, **67**, 7–14.
31 L. Liu, Z. Y. Gao, X. P. Su, X. Chen, L. Jiang and J. M. Yao, *ACS Sustainable Chem. Eng.*, 2015, **3**, 432–442.
32 A. Ali and S. Ahmed, *Int. J. Biol. Macromol.*, 2018, **109**, 273–286.
33 J. M. Dang and K. W. Leong, *Adv. Drug Delivery Rev.*, 2006, **58**, 487–499.
34 S. Bratskaya, S. Schwarz, J. Laube, T. Liebert, T. Heinze, O. Krentz, C. Lohmann and W. M. Kulicke, *Macromol. Mater. Eng.*, 2005, **290**, 778–785.
35 M. Rinaudo, *Prog. Polym. Sci.*, 2006, **31**, 603–632.
36 J. Li, H. Xiao, J. Li and Y. Zhong, *Int. J. Pharm.*, 2004, **278**, 329–342.
37 L. Shen and M. K. Patel, *J. Polym. Environ.*, 2008, **16**, 154–167.
38 K. Alvani, X. Qi and R. F. Tester, *Starch/Staerke*, 2011, **63**, 424–431.
39 L. Dokic-Baucal, P. Dokic and J. Jakovljevic, *Food Hydrocolloids*, 2004, **18**, 233–239.
40 X. Qi and R. F. Tester, *Starch/Staerke*, 2018, **70**, 10–14.
41 N. Reddy, R. Reddy and Q. Jiang, *Trends Biotechnol.*, 2015, **33**, 362–369.
42 N. A. O'Connor, A. Abugharbieh, F. Yasmeen, E. Buabeng, S. Mathew, D. Samaroo and H.-P. Cheng, *Int. J. Biol. Macromol.*, 2015, **72**, 88–93.
43 M. Castro-Cabado, F. J. Parra-Ruiz, A. L. Casado and J. San Román, *Polym. Polym. Compos.*, 2016, **24**, 643–654.
44 D. Gyawali, P. Nair, Y. Zhang, R. T. Tran, C. Zhang, M. Samchukov, M. Makarov, H. K. W. Kim and J. Yang, *Biomaterials*, 2010, **31**, 9092–9105.
45 W. E. Hennink and C. F. van Nostrum, *Adv. Drug Delivery Rev.*, 2012, **64**, 223–236.
46 L. Hovgaard and H. Brøndsted, *J. Controlled Release*, 1995, **36**, 159–166.
47 A. J. Kuijpers, P. B. Van Wachem, M. J. A. Van Luyn, G. H. M. Engbers, J. Krijgsveld, S. A. J. Zaat, J. Dankert and J. Feijen, *J. Controlled Release*, 2000, **67**, 323–336.
48 A. Concheiro and C. Alvarez-Lorenzo, *Adv. Drug Delivery Rev.*, 2013, **65**, 1188–1203.
49 G. Crini and M. Morcellet, *J. Sep. Sci.*, 2002, **25**, 789–813.
50 Y. Nobuhiko, N. Jun, O. Teruo and S. Yasuhisa, *J. Controlled Release*, 1993, **25**, 133–143.
51 M. Komiyama and H. Hirai, *Polym. J.*, 1987, **19**, 773–775.
52 L. L. H. Huang, P. C. Lee, L. W. Chen and K. H. Hsieh, *J. Biomed. Mater. Res.*, 1998, **39**, 630–636.
53 S. Suye and A. Mizusawa, *Sen'i Gakkaishi*, 1999, **55**, 73–77.
54 C. Rodriguez-Tenreiro, C. Alvarez-Lorenzo, A. Rodriguez-Perez, A. Concheiro and J. J. Torres-Labandeira, *Pharm. Res.*, 2006, **23**, 121–130.
55 Y. Nobuhiko, O. Teruo and S. Yasuhisa, *J. Controlled Release*, 1992, **22**, 105–116.
56 A. C. Stijnman, I. Bodnar and R. Hans Tromp, *Food Hydrocolloids*, 2011, **25**, 1393–1398.